Theoretical Study of the Structure and Bonding in Phosphatrane Molecules

V. Galasso*

Dipartimento di Scienze Chimiche, Università di Trieste, I-34127 Trieste, Italy

Received: December 16, 2003

The molecular structures of a representative selection of phosphatranes were studied by means of the ab initio MP2 method. The calculated results reasonably matched the available X-ray data. The special properties of the intrabridgehead interaction were described in terms of hybridization, bond order index, force constant, and vibrational frequency. The atom-in-molecules analysis of the electronic charge density showed the presence of a CP(3,−1) betwen the bridgehead centers in the cationic species but not in all of the neutral phosphatranes. The proton affinities of bases with no apical substituent on the phosphorus were accurately calculated for both the gas phase and solution (DMSO). The unique electronic structure of phosphatranes was theoretically investigated by means of their spectroscopic properties. The NMR chemical shifts and indirect nuclear spin−spin coupling constants, computed by DFT-based methods, were fairly consistent with experimental evidence, in particular for the observables involving the central phosphorus. The photoelectron spectrum of azaphosphatrane, having NMe equatorial groups, was interpreted by means of ab initio outer valence Green's function calculations, which gave a consistent reproduction of the energies and splittings of the uppermost bands, associated with the lone pairs of the bridgehead and equatorial heteroatoms. Thus, computations provided reliable predictions of the variations of the NMR parameters and ionization energies with change of the equatorial centers and apical substitution at phosphorus.

Introduction

Phosphatranes, also referred to as Verkade's bases, are football-shaped molecules of C_3 symmetry that display unusual structures, spectroscopic properties, and reactivities, including catalysis.[1−5] Furthermore, they are very strong bases due to the extraordinary stability of their protonated species.[1−7] From a qualitative standpoint, these features can be attributed to the partial bonding between the bridgehead phosphorus and axial nitrogen (N_{ax}) inside the caged structure. In this paper, extensive theoretical interest is devoted to phosphatranes **1**−**3**, $ZP[E(CH_2)_2]_3N$ with E = NH, NMe, and O, and Z = H^+, O, S, CH_3^+, and BH_3.

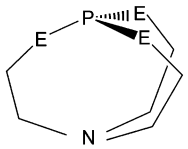

1 E = NH
2 E = NMe
3 E = O

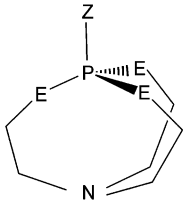

1(Z = H^+, O) E = NH
2(Z) E = NMe
3(Z) E = O
Z = H^+, O, S, CH_3^+, BH_3

The most noteworthy structural aspect of these molecules is the strong dependence of the intrabridgehead P--N_{ax} distance on the nature of the apical (Z) and equatorial (E) groups bound to phosphorus. This distance, which can formally be compared with the sum of the van der Waals radii, 3.35 Å, the sum of the covalent radii, 1.80 Å, and the standard length of a P−N single bond, 1.71 Å, is an insightful monitor of the unique electronic structure of these molecules. Following Verkade's suggestion,[1] these molecules could be qualitatively differentiated among pro-atranes **A** (with tetrahedral P, outwardly pyramidalized N_{ax}, and no intrabridgehead bond), quasi-atranes **B** (with tetrahedral P, planar N_{ax}, and weak intrabridgehead bond), and atranes **C** (with trigonal-bipyramidal P, inwardly pyramidalized N_{ax}, and effective intrabridgehead bond). Schematically, **A** and **B** display a bicyclic model, whereas **C** has a normal tricyclic arrangement.

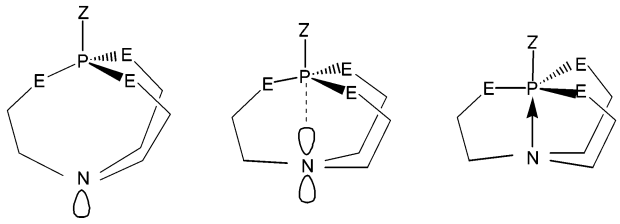

pro-atrane **A** quasi-atrane **B** atrane **C**

A cursory glance at the available X-ray data[7−14] provides the following picture. Compounds **2**(Z) and **3**(Z), with the apical Z group different from CH_3, may be formally characterized as quasi-atranes. They have longer P--N_{ax} distances, which range from 3.098 Å in **3**(BH_3) to 3.250 Å in **2**(S). The protonated bases **1**−**3**, with *r*(P--N_{ax}) varying from 1.967 Å in **2**$(H)^+$ to 2.077 Å in **1**$(H)^+$, should belong to the atrane case. The methylated cation **2**$(CH_3)^+$, with the intermediate distance of 2.772 Å, should be near the borderline for changeover from quasi-atrane to atrane structures. Finally, according to our theoretical results (vide infra), the free unsubstituted bases **1**, **2**, and **3** may be associated with the quasi-atrane group.

Because of the intimate interrelation between geometric and electronic structures, a systematic theoretical investigation into

* E-mail: galasso@univ.trieste.it.

10.1021/jp031324n CCC: $27.50
Published on Web 04/24/2004

the structural and spectroscopic properties of these molecules seemed timely. Here, we describe ab initio calculations of the equilibrium structures, proton affinities, and ionization energies, and density functional theory (DFT) calculations of the NMR chemical shifts and indirect nuclear spin−spin coupling constants. It must be mentioned that the structures and the proton affinities of a series of azaphosphatranes of the form $ZP[NR(CH_2)_2]_3N$ were analyzed at the ab initio Hartree−Fock (HF) level by Windus et al.[15] Furthermore, Nyulászi et al.[16] calculated the DFT and MP2 structure of the free base **1** and the DFT structure of the parent congener **2**. However, the present study covers a broader series of molecules $ZP[E(CH_2)_2]_3N$ at a higher theoretical level (ab initio MP2 for the equilibrium structures), and also investigates their NMR and photoelectron properties.

Computational Details

Second-order Møller−Plesset (MP2) full geometry optimizations employed the 6-31G(d) basis set with the Gaussian 98 suite of programs.[17] Harmonic frequency calculations were performed for all of the optimized structures, to establish that the stationary points are the correct minima. The force constant extraction and normal-mode analysis were then obtained by using the Wilson FG matrix method,[18] using standard internal coordinates and including the intrabridgehead interaction as an individual coordinate. Localization of the molecular orbitals was performed according to the Pipek−Mezey procedure,[19] and bond order indices were calculated from the definition of Sannigrahi and Kar.[20] The critical-point (CP) analyses of the scalar fields ρ and $\nabla^2\rho$ were carried out according to Bader's atom-in-molecules (AIM) theory.[21]

The ^{1}H, ^{13}C, and ^{31}P NMR absolute shielding constants (σ values) were calculated at the B3LYP/DFT level with the continuous set of gauge transformations (CSGT) method,[22] using the basis sets of Schäfer et al.,[23] TZP for H and TZ2P for the heavy atoms. The calculated magnetic shieldings were converted into the δ chemical shifts by noting that at the same level of theory the ^{1}H and ^{13}C absolute shieldings in TMS are 31.45 and 178.95, respectively, and the ^{31}P absolute shielding in PH_3 is 586.52.

The indirect nuclear spin−spin coupling constants were obtained by means of standard response-theory methods at the B3LYP/DFT level using the Dalton software.[24] For all of the examined molecules the Fermi contact contributions to the ^nJ(XY)s were calculated using the cc-pVDZ basis set.[25]

The vertical ionization energies (E_i's) of the free bases **1**−**3** were calculated at the ab initio level according to the outer valence Green's function (OVGF) method,[26] which incorporates the effects of electron correlation and reorganization beyond the Hartree−Fock approximation. The self-energy part was expanded up to third order, and the contributions of higher orders were estimated by means of a renormalization procedure. To calculate the self-energy part, all occupied valence molecular orbitals (MOs) and the 60, 79, and 55 lowest virtual MOs were considered for **1**, **2**, and **3**, respectively. The DZP basis set[27] was used for all three molecules.

Results and Discussion

Molecular Structures. Previous calculations at various levels of theory have shown that the computed structures of main group atranes are very sensitive to the inclusion of electron correlation.[15,16,28,29] Specifically, for some representative phosphatranes, both HF and DFT/B3LYP methods[13,29] gave intrabridgehead P--N_{ax} distances considerably longer than the X-ray values. A better agreement between theoretical and experimental values was obtained from MP2 computations.[13,29] Therefore, the ab initio MP2 procedure was here adopted for all molecules. Selected MP2 structural parameters, together with the available X-ray data,[7−14] are presented in Table 1. Even at this level of theory, a few remarkable discrepancies between theory and experiment occur for some cationic species: Δr(P--N_{ax}) = 0.07 Å for **2**(H)$^+$, 0.11 Å for **3**(H)$^+$, and 0.16 Å for **2**$(CH_3)^+$. The correlation between theory and experiment is instead reasonable for the other molecules. In this respect, it is worth mentioning that for some structurally related molecules, namely silatranes, the corresponding intrabridgehead Si--N_{ax} distance significantly changes with the physical state of the compounds.[30] Indeed, in fluoro- and methylsilatrane, isoelectronic and isostructural to **3**$(CH_3)^+$, the distance is 2.04 (Z = F) and 2.18 (Z = CH_3) Å in the crystalline state (X-ray determinations),[31,32] whereas it is 2.32 (F) and 2.45 (CH_3) Å in the gas phase (electron-diffraction experiments).[31,33] Thus, taking this case for granted, the crystal-packing forces may also be responsible for some strengthening of the P--N_{ax} interaction in the solid state of phosphatranes. Of course, the MP2 theoretical results mimic the gas-phase environment. As a matter of fact, our MP2 results for silatranes, 2.280 (F) and 2.411 (CH_3) Å, are close to the electron-diffraction values.

TABLE 1: Theoretical and Experimental Atrane and Axial Structural Parameters (Distances in Å, Sums of Bond Angles in deg)

	r(P--N_{ax})	r(P−Z)	$\sum\alpha$(ZPE)	$\sum\alpha$(EPE)	$\sum\alpha$($CN_{ax}C$)
1	3.027			313.3	358.2
1(H)$^+$	2.063	1.403	287.9	357.1	336.9
	2.077[a]	(*1.29*)	287.9	356.8	338.4
2	3.408			305.6	357.7
2(H)$^+$	2.034	1.396	283.6	358.1	337.3
	1.967[b]	(*1.41*)	285.0	358.8	333.0
3	3.283			307.2	358.1
3(H)$^+$	2.104	1.376	284.5	357.9	340.9
	1.986[c]	(*1.35*)	277.6	359.4	339.9
1(O)	2.693	1.502	327.5	329.3	350.9
2(O)	3.158	1.500	337.8	318.5	360.0
	3.140[d]	1.473	333.8	323.5	358.9
3(O)	3.111	1.477	339.9	316.2	359.7
2(S)	3.209	1.958	339.8	316.3	358.8
	3.250[e]	1.959	336.5	320.0	358.1
3(S)	3.137	1.908	341.2	314.6	359.5
	3.132[f]	1.933	332.5	324.2	357.5
2$(CH_3)^+$	2.614	1.823	312.0	343.0	351.5
	2.773[g]	1.810	316.0	339.3	354.6
3$(CH_3)^+$	2.196	1.795	291.1	355.5	341.9
2(BH_3)	3.170	1.924	338.3	318.0	360.0
3(BH_3)	3.088	1.886	338.6	317.6	359.9
	3.098[h]	1.884	334.6	322.1	359.1

[a] Reference 7. [b] Reference 8. [c] Reference 9. [d] Reference 10. [e] Reference 11. [f] Reference 12. [g] Reference 13. [h] Reference 14.

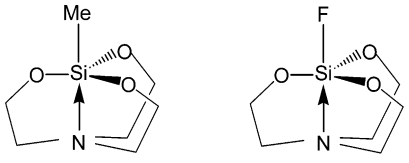

On the basis of this finding and the satisfactory agreement observed for r(P--N_{ax}) in the P-tetrahedral compounds **2**(O), **2**(S), **3**(S), and **3**(BH_3), the intrabridgehead distances computed for the parent bases **1** (3.03), **2** (3.41), and **3** (3.28 Å) should be reliable. Formal replacement of the NMe group by an O atom in the equatorial position, i.e., on passing from **2**(Z) to **3**(Z),

TABLE 2: Atrane and Axial Bonding Characteristics[a]

	bond	CP	r_c	ρ_c	$\nabla^2\rho_c$	boi	k	ω	PED
1	P--N_{ax}	(3,−1)	2.863	0.015	0.050	0.002	0.39	192	40
1$(H)^+$	P--N_{ax}	(3,−1)	1.517	0.085	0.012	0.345	0.85	384	42
	P−H	(3,−1)	1.234	0.179	0.068	0.954	3.69	2531	100
2	P--N_{ax}	(3,+3)	3.321	0.008	0.035	0.002	0.43	175	38
2$(H)^+$	P--N_{ax}	(3,−1)	1.478	0.090	0.016	0.366	0.87	416	40
	P−H	(3,−1)	1.229	0.182	0.091	0.993	3.81	2568	100
3	P--N_{ax}	(3,+3)	3.148	0.009	0.042	0.006	0.42	182	32
3$(H)^+$	P--N_{ax}	(3,−1)	1.608	0.083	−0.024	0.344	0.76	357	41
	P−H	(3,−1)	1.216	0.198	0.034	1.023	4.28	2729	100
1(O)	P--N_{ax}	(3,−1)	2.399	0.024	0.068	0.058	0.49	219	35
	P═O	(3,−1)	1.125	0.222	1.558	1.698	9.46	1216	84
2(O)	P--N_{ax}	(3,+3)	2.974	0.012	0.044	−0.004	0.37	139	40
	P═O	(3,−1)	1.124	0.223	1.517	1.683	9.40	1228	75
3(O)	P--N_{ax}	(3,+3)	2.937	0.012	0.049	0.014	0.41	165	22
	P═O	(3,−1)	1.114	0.235	1.719	1.835	10.66	1341	83
2(S)	P--N_{ax}	(3,+3)	3.043	0.011	0.042	−0.010	0.37	144	41
	P═S	(3,−1)	1.360	0.181	−0.378	1.558	4.32	751	49
3(S)	P--N_{ax}	(3,+3)	2.973	0.012	0.047	0.015	0.41	161	33
	P═S	(3,−1)	1.300	0.194	−0.283	1.689	5.23	822	53
2$(CH_3)^+$	P--N_{ax}	(3,−1)	2.340	0.031	0.063	0.126	0.45	229	23
	P−C	(3,−1)	1.258	0.179	−0.061	0.958	3.49	794	57
3$(CH_3)^+$	P--N_{ax}	(3,−1)	1.767	0.070	0.009	0.278	0.67	281	39
	P−C	(3,−1)	1.238	0.194	−0.062	0.996	3.92	838	69
2(BH_3)	P--N_{ax}	(3,−1)	2.999	0.012	0.044	−0.011	0.36	133	39
	P−B	(3,−1)	2.630	0.122	0.096	0.970	2.25	728	37
3(BH_3)	P--N_{ax}	(3,−1)	2.915	0.013	0.049	0.017	0.40	157	33
	P−B	(3,−1)	2.579	0.120	0.222	0.981	2.29	607	33

[a] r_c (in bohr), distance of the CP from the P atomic center; ρ_c (e $bohr^{-3}$) and $\nabla^2\rho_c$ (e $bohr^{-5}$), electron density and its Laplacian, respectively, at the CP; boi, bond order index; k (mdyn $Å^{-1}$), stretching force constant; ω (cm^{-1}), vibrational frequency; potential energy distribution (PED), % of the stretching coordinate in the vibrational mode.

results in a intrabridgehead distance shorter by 0.07−0.12 Å. A notable exception occurs for the methylated compounds, with the theoretical distance shortening by 0.41 Å from **2**$(CH_3)^+$ to **3**$(CH_3)^+$. Thus, **3**$(CH_3)^+$ is remarkably similar to the protonated bases. Indeed, monoprotonation of the parent bases **1**, **2**, and **3** causes a drastic shortening of the intrabridgehead distance. The MP2 calculations predict Δr(P--N_{ax}) = 0.97 Å in **1**, 1.38 Å in **2**, and 1.18 Å in **3**.

Another noteworthy point concerns the geometry at the two bridgehead atoms (Table 1). In the free bases **1**−**3** as well as in the P-tetracoordinate compounds **2**(Z) and **3**(Z), the P atom is pyramidal and N_{ax} is nearly planar. The inversion of the configuration at the P atom takes place upon protonation; hence, P becomes planar and N_{ax} upwardly pyramidalized. In turn, in the methylated species **2**$(CH_3)^+$ and **3**$(CH_3)^+$, consistent with their intermediate intrabridgehead distances, the sums of the bond angles at P and N_{ax} are in the direction of a stronger P--N_{ax} bonding than that predicted for the congener compounds **2**(Z) and **3**(Z). Finally, it is worth noting that, in agreement with the structural relationships reported for silatranes,[30] there is a strong correlation between the intrabridgehead P--N_{ax} distance and the deviation ΔP from coplanarity of the phosphorus and the three equatorial heteroatoms (MP2 theoretical values):

$$r(\text{P--N}_{ax}) = 2.0582\Delta P + 1.7643$$

(r and ΔP in Å; 15 points; correln coeff = 0.983)

To elucidate the nature of the P--N_{ax} interaction, an AIM analysis was performed on the MP2 electron density of each molecule. The critical point (CP) data are listed in Table 2: CP index; distance from the P nucleus, r_c; electron density, ρ_c; and Laplacian, $\nabla^2\rho_c$. As expected, a normal "bond" critical point, classified as CP(3,−1), is connected to the axial P−Z bond in all molecules. A unique picture cannot instead be depicted for the atrane P--N_{ax} interaction. Indeed, a "bond" CP(3,−1) is found for the protonated bases **1**$(H)^+$, **2**$(H)^+$, and **3**$(H)^+$, and for bases **1**, **1**(O), **2**(Z), and **3**(Z), with Z = CH_3^+ and BH_3. However, the P--N_{ax} densities ρ_c in the protonated bases **1**−**3** and **3**$(CH_3)^+$ are about 10 times larger than those in the neutral bases, suggesting that there is some dative P←N_{ax} bond in these molecules. Furthermore, since this CP(3,−1) is in each case much closer to the P nucleus, the associated bond is strongly polarized toward N_{ax}. In contrast, a local depletion of charge along the P--N_{ax} direction, i.e., a "cage" CP(3,+3), occurs for the free bases **2** and **3** and for compounds **2**(Z) and **3**(Z) with Z = O and S, indicating that there is not an effective P--N_{ax} bond in these molecules. On these grounds, no general and clear-cut answer can be given to the question of whether there is a intrabridgehead bond in this series of molecules.

To further characterize the P--N_{ax} interaction, other important bonding features are shown in Table 2: the intrabridgehead bond order index, stretching force constant, and vibrational frequency. The higher bond orders, about 0.35, as well as the larger force constants, about 0.8 mdyn/Å, are shown by the protonated bases **1**−**3**. Their intrabridgehead bond is twice as strong as that in the parent free bases. The latter are thus more flexible energetically with respect to a shortening/lengthening of the P--N_{ax} distance. The higher P--N_{ax} intrabridgehead stretching frequency is predicted at 416 cm^{-1} for **2**, whereas the lower frequency, 133 cm^{-1}, is computed for **2**(BH_3). The potential energy distribution shows that the contribution of the P--N_{ax} stretching coordinate to the associated IR mode varies from 22% in **3**(O) to 42% in **1**$(H)^+$.

Last, it is noteworthy that using the scale factor of 0.87 (obtained from a fit of the theoretical to experimental frequencies of PH_4^+ at the same level of theory), the stretching frequency for the apical P−H bond is predicted to be 2202 cm^{-1} in **1**$(H)^+$, 2234 cm^{-1} in **2**$(H)^+$, and 2374 cm^{-1} in **3**$(H)^+$, lower than the usual 2360−2430 cm^{-1} range of hydrophosphoranes.[34]

TABLE 3: Theoretical Proton Affinities (PAs in kJ mol^{-1}) and Phosphorus Lone Pair Properties in 1−3[a]

	PA(gas)	PA(DMSO)	hybridization	r_c	ρ_c	$\nabla^2\rho_c$
1	1128.4	1301.2	$sp^{0.68}$	1.412	0.151	−0.438
2	1152.1	1312.7	$sp^{0.62}$	1.409	0.153	−0.447
3	1034.9	1228.0	$sp^{0.46}$	1.400	0.157	−0.472

[a] r_c (in bohr), distance of the CP from the P atomic center; ρ_c (e bohr^{-3}) and $\nabla^2\rho_c$ (e bohr^{-5}), electron density and its Laplacian, respectively, at the CP.

Proton Affinities. Since **1**−**3** are known as very strong neutral bases,[1−7] it is worthwhile comparing their basicities. For this purpose, the gas-phase proton affinity (PA) was calculated at the MP2 level, by taking into account the zero-point energy (weighted by a factor of 0.89, as recommended)[35] and the basis set superposition error (estimated by the usual counterpoise method of Boys and Bernardi).[36] The theoretical results, reported in Table 3, indicate the basicity order **2** > **1** > **3**. Therefore, the substitution of the Me group for H at N_{eq} produces enhancement in basicity, in line with the alkyl-inductive effect and the observed shortening of the P--N_{ax} distance. This MP2 conclusion corroborates the previous HF result reported by Windus et al.[15] In contrast, the replacement of N_{eq} by the more electron-withdrawing O atom leads to reduction in PA. On the other hand, it is worth mentioning that the influence of the Z substituent on the basicity of **1** was recently studied by Koppel et al.[37] by DFT calculations on the model compounds **1**, **1**(NH), and **1**(CH_2).

According to the experimental pK_a values of the conjugated acids in DMSO solution, 29.6 calculated for **1** and 26.8 estimated for **2** by Laramay and Verkade,[7] **1** should be more basic than **2**. As a matter of fact, the pK_a of **2** in MeCN is 32.9.[6] No experimental pK_a is available for **3**. Since accurate predictions of PAs require careful treatment of both the solvation effects and the change in strain on protonation, these factors were also taken into account. In particular, the energetics of the protonation reaction in solution was calculated according to the isodensity surface polarized continuum model (IPCM)[38] with a dielectric constant of 45.0 (representing DMSO). However, the theoretical PAs in DMSO solution (Table 3) give the same order of the gas phase. Moreover, to get a relative estimate of the strain energies, use was made of the isodesmic reaction method, which proved useful for analyzing the basicity of proton sponges.[39] Thus, the strain energy of the free base is given by

$$P(E{-}CH_2{-}CH_2)_3N + 3CH_3CH_3 \rightarrow P(E{-}CH_2{-}CH_3)_3 + N(CH_2{-}CH_3)_3$$

and the strain energy of its protonated cation by

$$^{+}H{-}P(E{-}CH_2{-}CH_2)_3N + 3CH_3CH_3 \rightarrow {}^{+}H{-}P(E{-}CH_2{-}CH_3)_3 + N(CH_2{-}CH_3)_3$$

The calculated differences in strain energies are 86.5 (**1**, E = NH), 92.1 (**2**, E = NMe), and 74.2 kJ mol^{-1} (**3**, E = O). It can, therefore, be speculated that the change in strain on protonation does not play a significant role in determining the basicity sequence of these phosphatranes. In conclusion, a rationale for the puzzling discrepancy between the theoretical and experimental orders of basicity could be found in the deprotonation experiments on **1**(H)$^+$ reported by Laramay and Verkade:[40] "The results in toto strongly indicate that deprotonation of the P−H proton of cation **1**(H)$^+$ may in part be difficult because initial deprotonation occurs at an equatorial nitrogen, thereby strengthening the P−H bond owing to increased basicity of the phosphorus."

Last, as a further attempt to rationalize the gas-phase basic strengths of **1**−**3**, a CP analysis of properties of the P lone pair orbital (LPO) was performed according to Bader's AIM theory.[21] The relevant values of ρ_c and $\nabla^2\rho_c$, evaluated at the CP(3,−3) lying at the distance r_c from the P nucleus, as well as the composition of the P LPO, are also given in Table 3. Of particular relevance is the observation that the properties of the P LPO are not simply linked with basis strength. In this respect, it can be mentioned that a similar situation was encountered for substituted phosphines.[41]

Chemical Shifts. The most relevant results of the present calculations for the chemical shifts are reported in Table 4. It must be noted that highly accurate predictions of the δ(X) observables, in particular $\delta(^{31}P)$, require very large basis sets and sophisticated treatment of electron correlation effects.[44−47] Furthermore, another critical point concerns the ^{31}P shielding scale. Indeed, the standard reference compound for ^{31}P is 85% aqueous H_3PO_4, whose shielding cannot be accurately estimated by theory. A more convenient reference is PH_3, but its gas-to-liquid shift as large as 28 ppm[47] must be also taken into account. Therefore, following the suggestion advanced recently by van Wüllen,[48] the ^{31}P absolute magnetic shielding calculated for a substance S was here converted to the chemical shift relative to 85% H_3PO_4 by using the relation

$$\delta(S,calc) = \sigma(PH_3,calc) - \sigma(S,calc) - 266.1$$

where −266.1 is the gas-phase chemical shift of PH_3.[48] Thus, the DFT−CSGT results (Table 4) reasonably account for the experimental condensed-phase values. The mean absolute error is ∼9 ppm in a range as large as 164 ppm, and a gas-to-liquid shift of ∼10 ppm cannot be ruled out for the present molecules. Also, the main trends in the ^{31}P chemical shifts are consistently predicted. In particular, the extreme cases **1**(H)$^+$ (most shielded value −42.9) and **2** (less shielded value 120.8), the downfield displacement with the sequence Z = H^+, O, CH_3^+, S, and BH_3 in the **2**−**3**(Z) series, and the strong shielding of ∼130 ppm caused by protonation, i.e., on going from **1**−**3** to **1**−**3**(H)$^+$, are fairly reproduced by theory. Of course, the large movement of the ^{31}P resonance within the series of molecules reflects the complex interplay of many stereoelectronic factors—the change of geometry, disappearance of the P lone pair, replacement of the equatorial groups and apical substitution—which one can hardly disentangle. Other important NMR features of phosphatranes are the low-field $^1H(-P)$ signal of the protonated bases **1**−**3**(H)$^+$ and the high-field ^{13}C peak of the methylated bases **2**(CH_3)$^+$ and **3**(CH_3)$^+$. It is very satisfying to remark that the DFT−CSGT chemical shifts compare quite favorably with the available spectroscopic data. Furthermore, for all molecules, the overall agreement between theoretical and experimental $\delta(^{13}C)$ values is very good. Thus, on the whole, the theoretical predictions for the chemical shifts lends further support to the MP2-optimized structures. Finally, it is worthwhile stressing that the high-field ^{31}P chemical shift cannot be unambiguously attributed to the presence of a five-coordinate phosphorus. For example, **3**(O) has $\delta(^{31}P)$ of −6.6, only 4 ppm downfield from **2**(H)$^+$, which contrasts sharply with the large difference in the intrabridgehead distance: according to theory, 3.111 Å in **3**(O) versus 2.034 Å in **2**(H)$^+$. As a matter of fact, use of the appropriate theoretical data provides a weak

TABLE 4: NMR Chemical Shifts, $\delta(^{31}P)$ Relative to PH_3, and $\delta(^{13}C)$ and $\delta(^{1}H)$ Relative to TMS

	δ(P)		δ(Z)		δ(ECC)		δ(ECC)		δ(Me)[a]	
	theor	expt	theor	expt	theor	expt	theor	expt	theor	expt
1	99.1	89.3[b]			38.3		55.3			
1$(H)^+$	−63.4	−42.9[c]	5.6	5.6	33.9	34.2	51.5	50.6		
2	117.0	120.8[d]			50.8	49.4	51.4	51.3	34.5	37.2
2$(H)^+$	−22.0	−10.6[e]	5.1	5.2	41.5	41.3	48.5	47.3	34.4	34.4
3	122.2	115.2[f]			59.6		52.5			
3$(H)^+$	−17.5	−20.9[f]	6.5	6.0	59.5	60.0	48.9	48.5		
1(O)	19.3	21.3[c]			42.0	42.8	55.5	53.6		
2(O)	17.7	20.3[d]			54.8	49.5	53.6	51.4	35.1	35.0
3(O)	−10.8	−6.6[f]			67.7	65.9	53.7	49.0		
2(S)	77.6	75.9[d]			54.9	50.0	53.7	51.6	36.0	36.2
3(S)	58.9	60.9[f]			67.2	67.7	53.5	50.8		
2$(CH_3)^+$	35.1	48.3[g]	13.5	12.6	50.4	49.2	52.1	49.6	35.1	35.7
3$(CH_3)^+$	25.7		13.3		61.0		49.3			
2(BH_3)	103.3	98.8[h]			53.5		53.4		35.4	
3(BH_3)	118.1	98.3[f]			64.5	64.9	52.9	49.4		

[a] Me stands for the carbon nucleus of the methyl group. [b] Reference 7. [c] Reference 40. [d] Reference 42. [e] Reference 8. [f] Reference 43. [g] Reference 13. [h] Reference 11.

TABLE 5: NMR Nuclear Spin−Spin Coupling Constants (Hz)

	J(P--N_{ax})	^1J(PZ)		^1J(PE)	^2J(PC)		^2J(PMe)[a]		^3J(PC)	
	theor	theor	expt	theor	theor	expt	theor	expt	theor	expt
1	−0.3			42.0	−3.1				0.6	
1$(H)^+$	−1.1	396.2	453.0[b]	−28.0	2.0				7.9	11.1
2	0.6			53.3	−1.9		40.0	41.0[c]	2.0	
2$(H)^+$	0.7	416.5	491.0[d]	−20.6	6.5	6.1	14.3	17.1	6.4	7.3
3	0.6			146.5	−5.6				1.7	
3$(H)^+$	8.2	762.3	779.6[e]	135.0	−9.9	|10.8|			14.0	12.8
1(O)	0.9	119.1		−11.7	−2.4				−0.9	2.0[f]
2(O)	−0.6	125.2		−39.2	7.1		8.8	3.7[c]	−1.2	
3(O)	−0.5	154.9		106.1	−6.6	|8.9|[e]			−0.2	
2(S)	−0.8	−97.7		−25.4	5.3		12.3	5.2[c]	−1.2	
3(S)	−0.5	−125.0		124.5	−8.4	|11.8|[e]			−0.1	
2$(CH_3)^+$	3.3	126.3	132.5[g]	−16.4	5.4	3.6	6.7	4.7	3.6	
3$(CH_3)^+$	6.8	187.9		138.2	−9.7				11.5	
2(BH_3)	0.1	100.0	142.4[h]	6.9	1.6		14.5		0.4	
3(BH_3)	0.3	83.6	120.3[e]	148.8	−8.2	|10.8|			1.2	2.0

[a] Me stands for the carbon nucleus of the methyl group. [b] Reference 7. [c] Reference 42. [d] Reference 8. [e] Reference 43. [f] Reference 40. [g] Reference 13. [h] Reference 11.

correlation between these two parameters:

$$\delta(^{31}P) = 93.375[r(P\text{--}N_{ax})] - 217.914$$

(r in Å; 15 points; correln coeff = 0.777)

Therefore, caution should be used in interpreting this NMR parameter as a univocal monitor of the intrabridgehead bonding.

Indirect Nuclear Spin−Spin Coupling Constants. The results of the DFT calculations are presented in Table 5. Before the discussion is started, some preliminary comments are in order. First, highly accurate predictions of the J property require very large basis sets, in particular for the Fermi contact (FC) term, and more sophisticated exploitation of electron correlation effects.[49−51] Second, a full calculation of the J tensor involves all four contributions of the nonrelativistic Ramsey theory,[52] i.e., in addition to the FC term, also the diamagnetic spin−orbit (DSO), paramagnetic spin−orbit (PSO), and spin-dipole (SD) terms. However, by using the DFT/B3LYP perturbational approach, Helgaker et al.[53] have reported a satisfactory reproduction of a variety of ^nJ(XY) values. Furthermore, the predominance of the FC contribution to ^nJ(PX) in the present molecules is shown by our full DFT calculations for $^1J(PN_{eq})$ (FC = 41.97 Hz, noncontact = 4.53 Hz) of **1**, ^1J(PH) (762.31, −0.06) and $^1J(PO_{eq})$ (134.96, 15.96) of **3**$(H)^+$, ^1J(PC) (187.90, −2.84) of **3**$(CH_3)^+$, and ^1J(PB) (83.63, −4.27) of **3**(BH_3). Consequently, the heavy calculations of the noncontact contributions to ^nJ(PX) values of the investigated phosphatranes were omitted.

In the pattern of the ^nJ(XY) computed for phosphatranes (Table 5), the following aspects are remarkable. A small value of $J(^{31}P^{15}N_{ax})$ is predicted in all cases, which manifests the long-range rather than one-bond coupling between the bridgehead nuclei, i.e., ^4J instead of ^1J. Thus, it is significantly smaller than the value of 59 Hz of the normal, covalent P−N bond in $P(NMe_2)_3$.[54]

Consistent with naive expectation, the one-bond coupling constants between phosphorus and equatorial nuclei, $^1J(^{31}P^{15}N)$ and $^1J(^{31}P^{17}O)$, show a strong dependence upon the coordination state of P and nature of the apical Z substituent. Thus, the calculated $^1J(PN_{eq})$ changes from 53 Hz in **2** to −39 Hz in **2**(O), in line with the 59 and −27 Hz measured for the related acyclic species $P(NMe_2)_3$ and $O{=}P(NMe_2)_3$, respectively.[54] Likewise, the calculated $^1J(PO_{eq})$ of **3**, 147 Hz, and **3**(O), 106 Hz, resemble the experimental constants of $P(OMe)_3$ and $O{=}P(OMe)_3$, 154 and 90 Hz, respectively.[55]

The calculated geminal ^2J(PC) and vicinal ^3J(PC) coupling constants are in satisfactory agreement with the available spectroscopic data. It is well-known[56] that the value and sign of $^2J(PNC)$ are mainly dictated by the orientation of the N LPO, which acts as a transmitter of the coupling. For **2** and **2**$(H)^+$,

the DFT parameters compare quite favorably with the spectroscopic values, which further corroborates the reliability of their theoretical structures.

Of primary interest is the one-bond coupling constant over the apical bond, ^1J(PZ). The agreement between the DFT estimates and available experimental values for ^1J(PH) of **1**−**3**(H)$^+$ and ^1J(PC) of **2**,**3**(CH$_3$)$^+$ is satisfactory. A sizable underestimation is instead found for ^1J(PB) of **2**,**3**(BH$_3$), in which the role of electron correlation and the basis set flexibility are expected to be very important. Specifically, the experimental ^1J(PB) and ^1J(PC) constants >100 Hz clearly indicate the presence of a strong coordination bond between phosphorus and boron or carbon. On the other hand, the DFT predictions of ^1J(P═O) in **2**(O) and **3**(O) are close to the experimental values of the related systems O═P(NMe$_2$)$_3$ and O═P(OMe)$_3$, 145 and 165 Hz, respectively.[54,55]

The ^1J(PH) constant displays a wide range of 327 Hz across the series **1**−**3**(H)$^+$. The experimentally observed trend **1**(H)$^+$ < **2**(H)$^+$ < **3**(H)$^+$, fairly reproduced by theory, reflects the increasing s-character of the hybrid orbital of P in the P−H bond: 30% in **1**(H)$^+$, 31% in **2**(H)$^+$, and 41% in **3**(H)$^+$.

Ionization Energies. The most peculiar electronic aspect of the free bases **1** and **2** concerns the energy pattern of the five nonconjugatively connected LPOs, four *n*(N) and one *n*(P). From a qualitative standpoint, these semilocalized *n* MOs are energetically split by a mediated interplay of through-bond and through-space interactions, dictated by the molecular framework. Thus, the HOMO and HOMO−1 of **1** and **2** can simply be described as the out-of-phase n_-(N$_{ax}$,P) and in-phase n_+(N$_{ax}$,P), respectively, combinations of the P and N$_{ax}$ LPOs. The larger contribution is provided by N$_{ax}$ in the HOMO and by P in the HOMO−1, but minor contributions are also given by the N$_{eq}$ LPOs. Owing to symmetry constraints, the three N$_{eq}$ LPOs give rise to a pair of degenerate out-of-phase combinations n_-(N$_{eq}$) and the in-phase combination n_+(N$_{eq}$). In turn, these two uppermost valence MOs, of symmetry e and a, are to some extent admixed with the P and N$_{ax}$ LPOs. In the case of **3**, the picture is more complex, since it encompasses n_-(N$_{ax}$,P), n_+(N$_{ax}$,P), and the formally n_s and n_p LPOs of each of the three O atoms. However, since the energy gap between the pair n_-(N$_{ax}$,P)/n_+(N$_{ax}$,P) and the manifold of the *n*(O)'s is rather large (>1.5 eV), the discussion can be safely restricted to the ionizations out of the two uppermost valence MOs of **3**.

Of the free bases **1**−**3**, only for **2** the photoelectron (PE) spectrum has been reported, together with a qualitative assignment based on the naive Koopmans' theorem.[16] In the 6−12 eV region, **2** shows four distinct bands. The first, sharp band, centered at 6.61 eV, arises from one photoionization. The second, prominent broad band, peaked at 8.0 eV, is generated by three photoionizations. The third band, with maximum at 9.54 eV, is yielded by one ionization process, and the next broad band, with onset at 10.5 eV, corresponds to ionizations out of the σ outer valence MOs.

The ab initio OVGF E_i's, pole strengths, and assignments for bases **1**−**3** are reported in Table 6. Worth mentioning is that the pole strengths calculated for all of the investigated photoionization processes are larger than 0.90, which indicates the validity of the one-particle picture of ionization.[57] For **2**, the agreement between the OVGF estimates and the experimental data is good and allows a detailed interpretation of its PE spectrum. Thus, the first band is associated with n_-(N$_{ax}$,P), the second with the near-lying n_+(N$_{ax}$,P) and n_-(N$_{eq}$) (according to theory, separated by only 0.25 eV), the third with n_+(N$_{eq}$), and the fourth with σ MOs. Furthermore, owing to the good reproduction of the PE data of **2**, the OVGF results may be regarded as plausible candidates for the outer valence E_i's of the unstable species **1** and **2**.

TABLE 6: Vertical Ionization Energies (E_i's in eV), Pole Strengths (PS), and Assignments of 1−3

	assignment	PS	$E_{i,theor}$	$E_{i,expt}$
1	a[n_-(N$_{ax}$,P)]	0.92	6.88	
	a[n_+(N$_{ax}$,P)]	0.91	8.05	
	e[n_-(N$_{eq}$)]	0.91	9.01	
	a[n_+(N$_{eq}$)]	0.91	9.50	
	e(σ)	0.92	11.76	
2	a[n_-(N$_{ax}$,P)]	0.91	6.36	6.61[a]
	a[n_+(N$_{ax}$,P)]	0.91	7.75	8.0
	e[n_-(N$_{eq}$)]	0.91	8.06	8.0
	a[n_+(N$_{eq}$)]	0.91	9.52	9.54
	e(σ)	0.91	11.65	11.7
3	a[n_-(N$_{ax}$,P)]	0.92	7.66	
	a[n_+(N$_{ax}$,P)]	0.91	9.05	
	e[*n*(O)]	0.91	10.71	
	e[*n*(O)]	0.92	11.49	
	a[*n*(O)]	0.91	11.93	

[a] Reference 16.

The noteworthy features of the electronic structure of **2** are the following: (i) The exceptionally low value of the first E_i (<7 eV) is due to the sterically induced planarity of N$_{ax}$, its LPO being nearly pure p in character, the methyl destabilizing inductive effect, and the mixing of the (N$_{ax}$,P) LPOs, as previously discussed.[16] (ii) The second E_i, with the largest P contribution, is lower than the value 7.91 eV of the open-chain system P(NMe$_2$)$_3$.[58] (iii) The average value of the E_i[n(N$_{eq}$)]'s is 8.51 eV, with a splitting Δn(N$_{eq}$) of 1.5 eV. Correlation with the average E_i[*n*(N)] (8.41 eV)[59] of 1,4,7-triazatricyclo[5.2.1.0^{4,10}]-decane, having a cup-shaped structure of C_3 symmetry, evidences a similar balance of the competing electronic interactions transmitted across the apical center, CH in the tricyclic system and P in **2**.

Replacement of the NMe by the NH groups in **2** formally generates **1**. The PE spectrum of **1** should, therefore, be expected to bear a close resemblance to that of **2**, with a slight shift toward higher ionization energy due to relief of the methyl destabilizing inductive effect. According to the OVGF results (Table 6), this expectation is only partially confirmed. Indeed, both the HOMO and HOMO−1 are stabilized by 0.5 and 0.3 eV, respectively, but the next two valence MOs display substantial differences from **2**. These are brought about by the hybridization change of N$_{eq}$, which moves from the perfectly planar geometry in **2** to the pyramidal arrangement in **1** (the sum of the three angles at nitrogen becoming 341.5°). As a consequence, its LPO changes from pure p character in **2** to composition sp$^{2.70}$ in **1**. This stereoelectronic change is reflected in a net stabilization of the average n(N$_{eq}$), from 8.55 eV in **2** to 9.17 eV in **1**, and a concomitant reduction of Δn(N$_{eq}$), from 1.5 to 0.5 eV.

The considerable stereodependence of E_i[n(N$_{ax}$)] can best be shown by correlating the OVGF estimate of $E_{i,1}$ of **1** (6.88 eV) with the experimental $E_{i,1}$ values of related caged compounds. Indeed, it is similar to the value (7.13 eV)[60] of the isostructural manxine, N(CH$_2$CH$_2$CH$_2$)$_3$CH, which also contains a planar bridgehead nitrogen. It is instead 1 eV lower than the value of 1-azaadamantane (7.94 eV),[61] which has a pyramidal bridgehead nitrogen.

Upon formal replacement of the NMe groups by O atoms in the equatorial positions, i.e., on passing from **2** to **3**, both the HOMO and HOMO−1 are predicted by theory to be shifted 1.3 eV to higher binding energy, due to charge migration toward the O atoms. Correlation of the theoretical $E_{i,2}$−$E_{i,5}$ of **3** with

the experimental $E_{i,1}-E_{i,4}$ of the related acyclic species $P(OMe)_3$, with 9.25 n(P), 10.53 n(O), 11.16 n(O), and 12.24 n(O) eV,[58] indicates a destabilization of n(P) by ~0.2 eV and a concomitant stabilization of the n(O)'s by ~0.2 eV, as an overall result of cyclization. With reference to the OVGF results, the sequence **2** > **1** > **3** is exhibited by both $n_-(P,N_{ax})$ and $n_+(P,N_{ax})$, whereas their Δn varies as **2** ≈ **3** > **1**. Of course, it is tempting to look at $\Delta n_\pm(N_{ax},P)$ as an index of the strength of the intrabridgehead interaction. However, this attempt fails because the sequence of $\Delta n_\pm(N_{ax},P)$ is in strong conflict with the variation of $r(P\text{--}N_{ax})$, **1** < **2** < **3**.

The primary effect of the axial Z addition on the phosphorus of bases **1**−**3** is the elimination of n(P) and its conversion into a strongly bonding P−Z MO. According to our OVGF calculations, the uppermost $n(N_{ax})$ MO becomes more tightly bound than in the parent free bases: 7.32 eV in **2**(O), 7.40 eV in **2**(S), 7.22 eV in **2**(BH_3), 8.23 eV in **3**(O), 8.20 eV in **3**(S), and 8.28 eV in **3**(BH_3).

Concluding Remarks

A theoretical, detailed compendium of structural and spectroscopic data of a representative selection of phosphatrane molecules, having nitrogen or oxygen as equatorial centers, has been presented. The main interest has been devoted to the subtle intrabridgehead interaction between the bridgehead phosphorus and nitrogen atoms, the so-called atrane bonding. The molecular structure and bonding have been thoroughly investigated by the ab initio MP2 method. On the whole, the correspondence between theoretical results and X-ray available data is reasonable. The special properties of the atrane bonding have been comprehensively described in terms of hybridization of the bridgehead atoms, bond order index, force constant, and vibrational frequency. The analysis of the bond critical points according to the AIM theory has shown the presence of a CP(3,−1) between the bridgehead centers in the cationic species but not in all of the neutral phosphatranes. The proton affinities of bases with no apical substituent on the phosphorus have been accurately calculated for both the gas phase and solution (DMSO) and also described in terms of the CP analysis of the phosphorus lone pair. The computed basicity trend is **2** > **1** > **3**.

The unique electronic structure of phosphatranes has been further investigated with their NMR and PE spectroscopic properties. The computational results, obtained at the ab initio and DFT levels, have provided detailed complementary information, which makes up for the lack of experimental measurements. In particular, the stereodependence and substituent dependence of the variations in the ^{31}P NMR chemical shift as well as of the indirect nuclear spin−spin coupling constants has been satisfactorily accounted for by the DFT calculations. The ab initio OVGF results have yielded an accurate interpretation of the main features in the PE spectrum of phosphatrane **2**, i.e., nature, location, splitting, and sequence of the E_i's associated with the n LPOs of the bridgehead and equatorial heteroatoms. Thus, reasonably good predictions of the variations of these important E_i's for all of the neutral phosphatranes have been obtained from the OVGF procedure.

Acknowledgment. This work was supported by grants from MIUR of Italy. The author thanks Prof. T. Helgaker (University of Oslo) for kindly providing the Dalton computer package and Prof. J. G. Verkade (Iowa State University) for useful suggestions.

References and Notes

(1) Verkade, J. G. *Acc. Chem. Res.* **1993**, *26*, 483.
(2) Verkade, J. G.*Coord. Chem. Rev.* **1994**, *137*, 233.
(3) Tang, J.-S.; Verkade, J. G. *Synth. Methods Organomet. Inorg. Chem.* **1996**, *3*, 177.
(4) Verkade, J. G.; Kisanga, P. B. *Tetrahedron* **2003**, *59*, 7819.
(5) Verkade, J. G. *Top. Curr. Chem.* **2003**, *223*, 1.
(6) Kisanga, P. B.; Verkade, J. G. *J. Org. Chem.* **2000**, *65*, 5431.
(7) Laramay, M. A. H.; Verkade, J. G. *J. Am. Chem. Soc.* **1990**, *112*, 9421.
(8) Lensink, C.; Xi, S. K.; Daniels, L. M.; Verkade, J. G. *J. Am. Chem. Soc.* **1989**, *111*, 3478.
(9) Clardy, J. C.; Milbrath, D. S.; Springer, J. P.; Verkade, J. G. *J. Am. Chem. Soc.* **1976**, *98*, 623.
(10) Tang, J.; Mohan, T.; Verkade, J. G. *J. Org. Chem.* **1994**, *59*, 4931.
(11) Xi, S. K.; Schmidt, H.; Lensink, C.; Kim, S.; Wintergrass, D.; Daniels, L. M.; Jacobson, R A.: Verkade, J. G. *Inorg. Chem.* **1990**, *29*, 2214.
(12) Clardy, J. C.; Milbrath, D. S.; Verkade, J. G. *J. Am. Chem. Soc.* **1977**, *99*, 631.
(13) Mohan, T.; Arumugam, S.; Wang, T.; Jacobson, R. A.; Verkade, J. G. *Heteroat. Chem.* **1996**, *7*, 455.
(14) Clardy, J. C.; Milbrath, D. S.; Verkade, J. G. *Inorg. Chem.* **1977**, *16*, 2135.
(15) Windus, T. L.: Schmidt, M. W.; Gordon, M. S. *J. Am. Chem. Soc.* **1994**, *116*, 11449.
(16) Nyulászi, L.; Veszprémi, T.; D'Sa, B. A.; Verkade, J. G. *Inorg. Chem.* **1996**, *35*, 6102.
(17) Frisch, M. J.; Trucks, G. W.; Schlegel, H. B.; Scuseria, G. E.; Robb, M. A.; Cheeseman, J. R.; Zakrzewski, V. G.; Montgomery, J. A.; Stratmann, R. E.; Burant, J. C.; Dapprich, S.; Millam, J. M.; Daniels, A. D.; Kudin, K. N.; Strain, M. C.; Farkas, O.; Tomasi, J.; Barone, V.; Cossi, M.; Cammi, R.; Mennucci, B.; Pomelli, C.; Adamo, C.; Clifford, S.; Ochterski, J.; Petersson, G. A.; Ayala, P. Y.; Cui, Q.; Morokuma, K.; Malick, D. K.; Rabuck, A. D.; Raghavachari, K.; Foresman, J. B.; Cioslowski, J.; Ortiz, J. V.; Stefanov, B. B.; Liu, G.; Liasenko, A.; Piskorz, P.; Komaroni, I.; Gomberts, R.; Martin, R. L.; Fox, D. J.; Keith, T.; Al-Laham, M. A.; Peng, C. Y.; Nanayakkara, A.; Gonzales, C.; Challacombe, M.; Gill, P. M. W.; Johnson, B.; Chen, W.; Wong, M. W.; Andres, J. L.; C. Gonzales, C.; Head-Gordon, M.; Replogle, E. S.; Pople, J. A. *Gaussian 98*, revision A.6; Gaussian, Inc.: Pittsburgh, PA, 1998.
(18) Wilson, E. B.; Decius, J. C.; Cross, P. C. *Molecular Vibrations*; McGraw-Hill: New York, 1945.
(19) Pipek, J.; Mezey, P. G. *J. Chem. Phys.* **1989**, *90*, 4916.
(20) Sannigrahi, A. B.; Kar, T. *Chem. Phys. Lett.* **1990**, *173*, 569.
(21) Bader, R. F. W. *Atoms In Molecules; A Quantum Theory*; Oxford University Press: Oxford, 1990.
(22) Keith, T. A.; Bader, R. F. W. *Chem. Phys. Lett.* **1993**, *210*, 223.
(23) Schäfer, A.; Huber, C.; Ahlrichs, R. *J. Chem. Phys.* **1994**, *100*, 5829.
(24) Helgaker, T.; Jensen, H. J. Aa.; Jørgensen, P.; Olsen, J.; Ruud, K.; Aagren, H.; Auer, A. A.; Bak, K. L.; Bakken, V.; Christiansen, O.; Coriani, S.; Dahle, P.; Dalskov, E. K.; Enevoldsen, T.; Fernadez, B.; Haettig, C.; Hald, K.; Halkier, A.; Heiberg, H.; Hettema, H.; Jonsson, D.; Kirpekar, S.; Kobayashi, R.; Koch, H.; Mikkelsen, K. V.; Norman, P.; Packer, M. J.; Pedersen, T. B.; Ruden, T. A.; Sanchez, A.; Saue, T.; Sauer, S. P. A.; Schimmelpfennig, B.; Sylvester-Hvid, K. O.; Taylor, P. R.; Vahtras, O. *Dalton, a molecular electronic structure program*, release 2.0; University of Oslo: Oslo, Norway, 2002.
(25) Woon, D. E.; Dunning, T. H., Jr. *J. Chem. Phys.* **1993**, *98*, 1358.
(26) Cederbaum, L. S. *J. Phys. B* **1975**, *8*, 290.
(27) Dunning, T. H., Jr. *J. Chem. Phys.* **1970**, *53*, 2823.
(28) Anglada, J. M.; Bo, C.; Bofill, J. M.; Crehuet, R.; Poblet, J. M. *Organometallics* **1999**, *18*, 5584.
(29) Kobayashi, J.; Goto, K.; Kawashima, T.; Schmidt, M. S.; Nagase, S. *J. Am. Chem. Soc.* **2002**, *124*, 3703.
(30) Greenberg, A.; Wu, G. *Struct. Chem.* **1989**, *1*, 79.
(31) Parkanyi, L.; Hencsei, P.; Bihatsi, L.; Müller, T. *J. Organomet. Chem.* **1984**, *269*, 1.
(32) Parkanyi, L.; Bihatsi, L.; Hencsei, P. *Cryst. Struct. Commun.* **1978**, *7*, 435.
(33) Shen, Q.; Hilderbrandt, R. L. *J. Mol. Struct.* **1980**, *64*, 257.
(34) Brazier, J. F.; Houalla, D.; Loenig, M.; Wolf, R. *Top. Phosphorus Chem.* **1976**, *8*, 99.
(35) Hout, R. F.; Levi, B. A.; Hehre, W. J. *J. Comput. Chem.* **1982**, *3*, 234.
(36) Boys, S. F.; Bernardi, F. *Mol. Phys.* **1970**, *19*, 553.
(37) Koppel, I. A.; Schwesinger, R.; Breuer, T.; Burk, P.; Herodes, K.; Koppel, I.; Leito, I.; Mishima, M. *J. Phys. Chem. A* **2001**, *105*, 9575.
(38) Foresman, J. B.; Keith, T. A.; Wiberg, K. B.; Snoonian, J.; Frisch, M. J. *J. Phys. Chem.* **1996**, *100*, 16098.
(39) Howard, S. T. *J. Am. Chem. Soc.* **2000**, *122*, 8238.

(40) Laramay, M. A. H.; Verkade, J. G. *Z. Anorg. Allg. Chem.* **1991**, *605*, 163.
(41) Howard, S. T.; Platts, J. A. *J. Phys. Chem.* **1995**, *99*, 9027.
(42) Schmidt, H.; Lensink, C.; Xi, S. K.; Verkade, J. G. *Z. Anorg. Allg. Chem.* **1989**, *578*, 75.
(43) Milbrath, D. S.; Verkade, J. G. *J. Am. Chem. Soc.* **1977**, *99*, 6607.
(44) Fleischer, U.; Schindler, M.; Kutzelnigg, W. *J. Chem. Phys.* **1987**, *86*, 6337.
(45) Gauss, J. *Chem. Phys. Lett.* **1992**, *191*, 614.
(46) Wilson, P. J.; Amos, R. D.; Handy, N. C. *Mol. Phys.* **1999**, *97*, 757.
(47) Jameson, C. J.; De Dios, A.; Jameson, A. K. *Chem. Phys. Lett.* **1990**, *167*, 575.
(48) van Wüllen, C. *Phys. Chem. Chem. Phys.* **2000**, *2*, 2137.
(49) Helgaker, T.; Jaszuński, M.; Ruud, K.; Górska, A. *Theor. Chem. Acc.* **1998**, *99*, 175.
(50) Helgaker, T.; Jaszuński, M.; Ruud, K. *Chem. Rev.* **1999**, *99*, 239.
(51) Perera, S. A.; Nooijen, M.; Bartlett, R. J. *J. Chem. Phys.* **1996**, *104*, 3209.
(52) Ramsey, N. F. *Phys. Rev.* **1953**, *91*, 303.
(53) Helgaker, T.; Watson, M.; Handy, N. C. *J. Chem. Phys.* **2000**, *113*, 9402.
(54) Gray, G. A.; Albright, T. A. *J. Am. Chem. Soc.* **1976**, *98*, 3857.
(55) Christ, H. A.; Diehl, P. *Helv. Phys. Acta* **1962**, *36*, 170.
(56) Hargis, J. H.; Jennings, W. B.; Worley, S. D.; Tolley, M. S. *J. Am. Chem. Soc.* **1980**, *102*, 13.
(57) Deleuze, M. S. *J. Chem. Phys.* **2002**, *116*, 7012.
(58) Worley, S. D.; Hargis, J. H.; Chang, L.; Mattson, G. A.; Jennings, W. B. *J. Electron Spectrosc. Relat. Phenom.* **1982**, *25*, 135.
(59) Galasso, V.; Hansen, J.; Jones, D.; Mascal, M. *J. Mol. Struct. (Theochem)* **1997**, *392*, 21.
(60) Alder, R. W.; Arrowsmith, R. J.; Casson, A.; Sessions, R. B.; Heilbronner, E.; Kovač, B.; Huber, H.; Taagepera, M. *J. Am. Chem. Soc.* **1981**, *103*, 6137.
(61) Worrell, C.; Verhoeven, J. W.; Speckamp, W. N. *Tetrahedron* **1974**, *30*, 3525.